

## Research Article

# Spherical Pendulum Small Oscillations for Slewing Crane Motion

Alexander V. Perig,<sup>1</sup> Alexander N. Stadnik,<sup>2</sup> and Alexander I. Deriglazov<sup>2</sup>

<sup>1</sup> *Manufacturing Processes and Automation Engineering Department, Engineering Automation Faculty, Donbass State Engineering Academy, Shkadinova 72, Donetsk Region, Kramatorsk 84313, Ukraine*

<sup>2</sup> *Department of Technical Mechanics, Engineering Automation Faculty, Donbass State Engineering Academy, Shkadinova 72, Donetsk Region, Kramatorsk 84313, Ukraine*

Correspondence should be addressed to Alexander V. Perig; [olexander.perig@gmail.com](mailto:olexander.perig@gmail.com)

Received 29 August 2013; Accepted 2 October 2013; Published 9 January 2014

Academic Editors: N.-I. Kim, M. Seddeek, and M. Zappalorto

Copyright © 2014 Alexander V. Perig et al. This is an open access article distributed under the Creative Commons Attribution License, which permits unrestricted use, distribution, and reproduction in any medium, provided the original work is properly cited.

The present paper focuses on the Lagrange mechanics-based description of small oscillations of a spherical pendulum with a uniformly rotating suspension center. The analytical solution of the natural frequencies' problem has been derived for the case of uniform rotation of a crane boom. The payload paths have been found in the inertial reference frame fixed on earth and in the noninertial reference frame, which is connected with the rotating crane boom. The numerical amplitude-frequency characteristics of the relative payload motion have been found. The mechanical interpretation of the terms in Lagrange equations has been outlined. The analytical expression and numerical estimation for cable tension force have been proposed. The numerical computational results, which correlate very accurately with the experimental observations, have been shown.

## 1. Introduction

The solution of nonlinear differential equations for spherical pendulum swaying requires the introduction of modern numerical computational analysis techniques. Such computer techniques allow us to produce approximate solutions of the posed problems. However, the linearized models for spherical pendulum small swaying motion provide a clear mechanical explanation and the first numerical approximation of the complex spherical motion problems. This fact confirms the significance of the small oscillation problems for the modern field of lifting-and-transport machines. A series of modern research efforts [1–22] have been focused on the solution of a spherical pendulum with moving pivot center.

Abdel-Rahman and Nayfeh [1] have studied the dynamic problem for a “crane boom tip-payload” mechanical system focused on the reduction of payload lateral vibrations by reeling and unreeling the hoist cable. In this work, the authors have derived two- and three-dimensional models for a spherical pendulum taking into account the linearity of transport motion.

Adamiec-Wójcik et al. [2] have provided a numerical finite-element simulation of the supporting frame of an offshore crane portal construction. Within the proposed model, supporting frame elastic oscillations define both the payload motion and the displacements of the suspension center with a payload on the cable. The derived model also incorporates ship vibration motion.

Aston has obtained two independent motion equations for a spherical pendulum taking into account viscous friction effects. This model neglects the components of the Coriolis inertia force [3].

Betsch et al. [4] have described rotary crane dynamics in terms of redundant coordinates with an introduction of differential-algebraic equations (DAEs). The authors' approach focused on the simultaneous incorporation of a large total number of redundant coordinates and the augmentation constraints do not fully describe the particular cases of rotary crane dynamics.

Błajer and Kołodziejczyk [5] have derived governing DAE equations for the open-loop control formulation that forces the underactuated crane system to complete the partly

specified motion. It is necessary to note that this paper deals primarily with controlled in-plane motions of the crane system with linear transport motion. Blajer and Kołodziejczyk [6] have investigated the control of underactuated crane mechanical systems with servo constraints. This work takes into account the restoring load gravity force in the horizontal plane. However, the derived mathematical model assumes primarily linear transport motion without the Coriolis inertia force. Blajer and Kołodziejczyk [7] have presented a conceptual research article focused on the building of n-index DAE systems for a relevant dynamic description of partly specified crane system motion. Blajer and Kołodziejczyk [8] have introduced a carefully argued computational technique for numerical simulation of cranes based on the use of dependent coordinates. The advantages of dependent coordinates' usage have been outlined. It is necessary to note that with each new research effort, the authors apply much more sophisticated computational methods and derive more exact governing dynamic equations. However, this paper is also based on the same simple pendulum model as the first approaches, wherein the Coriolis inertia force and the restoring load gravity force are ignored. Blajer et al. [9] have simulated a two-tier framed human arm model with segments of equal length. The application of this model seems to be very useful for the dynamic analysis of a swaying load in the horizontal plane during rotation of a crane boom. Blajer and Kołodziejczyk [10] have developed improved DAE equations for more precise rotary crane dynamics simulation. But, additional dimensional analysis for the explicit forms of the governing equations would greatly enhance the work.

Cha et al. [11] have applied a topological modeling approach to a dynamic simulation of multiple floating cranes in shipyards taking into account crane boom oscillations.

Ellermann et al. [12] have introduced the vector of generalized gyroscopic and Coriolis forces for a mathematical description of nonlinear dynamics of floating cranes. This work used a comprehensive model with a set of 20 differential equations but does not allow proper analysis of particular cases of floating jib crane-load system motions.

Erneux and Kalmár-Nagy [13] have proposed a plane pendulum container crane model with linear transport trolley motion. This model illustrates linear displacement of the plane pendulum suspension center.

Glossiotis and Antoniadis [14] have derived a four-degrees-of-freedom (4DOF) model for the rotary crane system, incorporating both hoisting and slewing payload motions and thus is able to handle cases where hoisting can be simultaneously applied to the rotary motion.

Ibrahim [15] has studied the issues of multiplicative noise and noise-enhanced stability of spherical pendulums.

Kortelainen and Mikkola [16] have introduced data management techniques within an approach using a semantic data model for payload oscillation problems.

Mitrev [17] has applied his generalized approach with the introduction of an inertia force vector to the case of linear transport motion of the pendulum pivot center. Grigorov and Mitrev [18] have investigated a spherical pendulum dynamic model for a numerical solution of a freely suspended swinging load problem. They have derived absolute

trajectories of both the pendulum suspension center and the swinging load.

Osiński and Wojciech [19] have analyzed the hoist motion of a mechanical system consisting of a load, hoist rope, and elastic crane jib. This study mainly deals with rectilinear load oscillations and lateral crane jib vibrations.

Ren et al. [20] have used a mixed approach combining both analytical and finite-element techniques for the Lagrangian function of a mechanical system. They have determined the relations between load swaying, crane boom flexibility, and wave motions. Schaub [21] has implemented a rate-based ship-mounted crane payload pendulation control system. This research is focused on a kinematic approach to payload stabilization with an emphasis on the usage of inertial measurement unit (IMU) information.

Uchiyama [22] has applied control theory techniques for a robust crane controller design that provides robustness with respect to changes in cable length and transported payload mass without iterative computations.

At the same time, these known articles [1–22] do not do justice to load swaying descriptions using Coriolis effects in relative motion. The present paper focuses on these issues.

The present paper focuses on the Lagrange mechanics-based description of small oscillations for a spherical pendulum with a uniformly rotating suspension center.

The prime novelty statement of the present paper is based on the rational introduction of a Cartesian coordinate system for study of small relative swaying of a payload and substantiation of uniformity of crane boom rotation.

## 2. Kinematic Analysis

In order to solve the problem, we introduce the Lagrange equations for the motion of the mechanical system “crane boom  $BO_2$ -load  $M$ ” which is shown in Figure 1.

The computational scheme in Figure 1 may be described with an introduction of three degrees of freedom. For generalized coordinates, we assume the rectangular coordinates  $x$ ,  $y$ , and  $z$  of the load and the angle  $\varphi_e = \omega_e t$  of crane boom  $BO_2$  uniform rotation in the horizontal plane ( $xy$ ) with the constant angular velocity  $\omega_e$  around the vertical axis  $O_2z_2$ . We denote the fixed inertial coordinate system as  $x_2y_2z_2$  and the moving noninertial frame of reference as  $x_1y_1z_1$ , which is rigidly bounded with the crane boom  $BO_2$ . Rotation of the moving noninertial frame of reference  $x_1y_1z_1$  around the fixed inertial coordinate system  $x_2y_2z_2$  defines the transportation motion. The motion of load  $M$  relative to the moving noninertial frame of reference  $x_1y_1z_1$  defines the relative motion.

The scalar of the load  $M$  transportation velocity is defined as  $V_e = \omega_e \cdot O_2M$ , and transportation velocity vector  $\mathbf{V}_e$  is perpendicular to  $\mathbf{O}_2\mathbf{M}$ , that is, the scalar product  $(\mathbf{V}_e, \mathbf{O}_2\mathbf{M}) = 0$  (Figure 1). The relative velocity vector  $\mathbf{V}_r$  of the load  $M$  is defined as  $\mathbf{V}_r = (dx_1/dt, dy_1/dt, dz_1/dt)$  in Figure 1. In the initial time  $t = 0$ , load  $M$  has the vertical  $BA_{st}$  in-line position; that is, the load  $M$  initial position coincides with the static equilibrium position  $A_{st}$  for the load  $M$  on the cable  $MB$ .

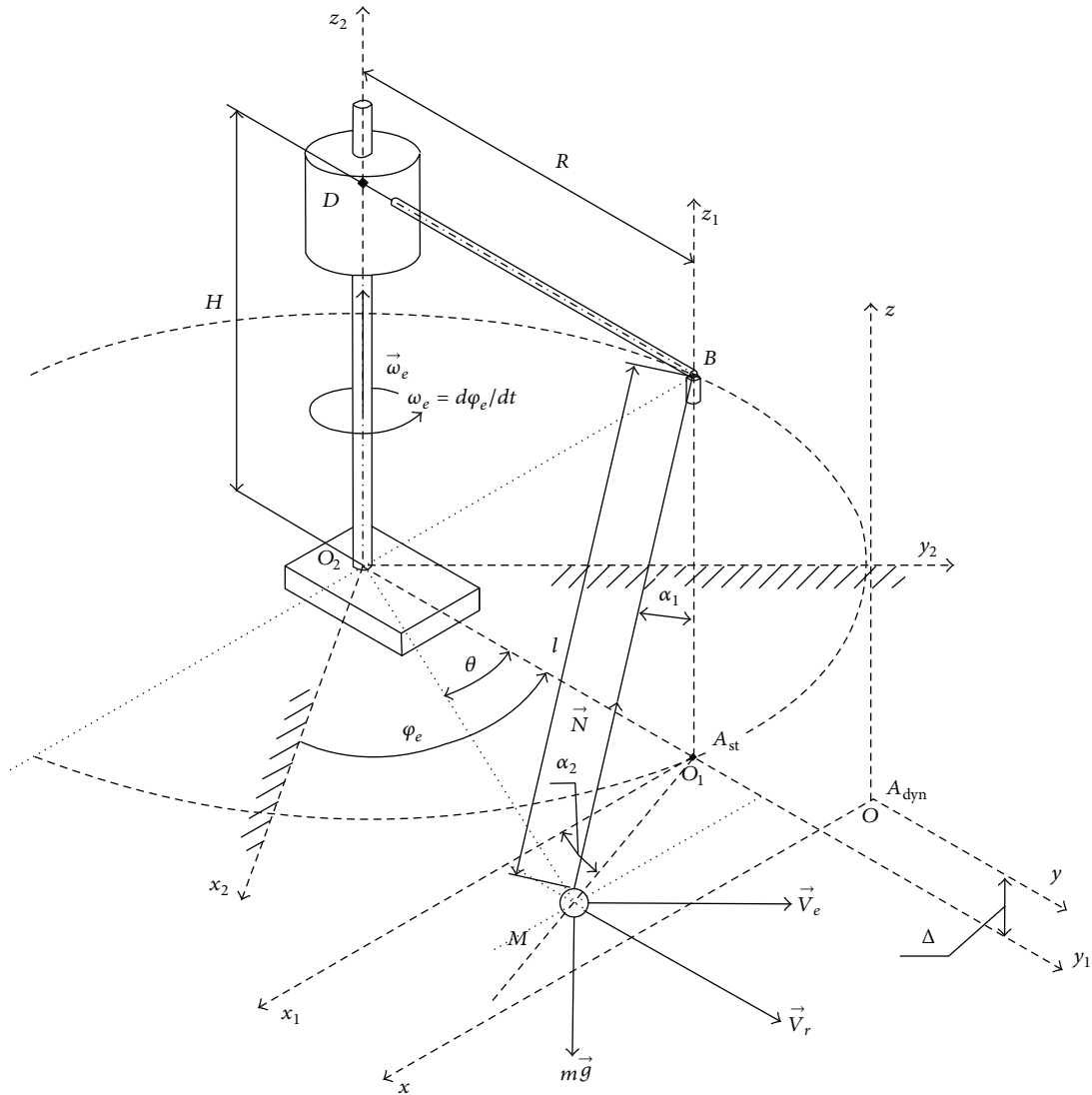


FIGURE 1: Computational spatial scheme of spherical pendulum  $M$ , swaying on the cable  $MB$  during crane boom  $BO_2$  slewing motion for the linearized model derivation in Cartesian coordinates.

At time  $t = 0$ , the load  $M$  has zero absolute velocity and the initial relative velocity is  $V_{rx}(0) = +\omega_e \cdot BD$  (Figure 1). In Figure 1, we denote the angle  $\theta$ , which is the current angle  $A_{st}O_2M$ , that is, the angle between the axis  $y_1$  and the radius-vector  $O_2M$ , where  $\sin(\theta) = x_1/O_2M$ ;  $\cos(\theta) = (R+y_1)/O_2M$ . The vertical coordinate  $z_1$  in Figure 1 is defined as  $z_1 = l - l \cdot \cos(\alpha_1)$ , where  $\alpha_1$  is the angle between the cable  $MB$  and the vertical.

For small angles  $\alpha_1$ , the projections of the absolute velocity vector may be written as

$$\begin{aligned} V_{x_1} &= \left( \frac{dx_1}{dt} \right) - V_e \cdot \cos(\theta), \\ V_{y_1} &= \left( \frac{dy_1}{dt} \right) + V_e \cdot \sin(\theta), \\ V_{z_1} &= \left( \frac{dz_1}{dt} \right) = \left( \frac{d\alpha_1}{dt} \right) \cdot l \cdot \sin(\alpha_1). \end{aligned} \quad (1)$$

Taking into account Figure 1, the system of (1) for the projections of the absolute velocity vector takes the following form:

$$\begin{aligned} V_{x_1} &= \left( \frac{dx_1}{dt} \right) - \left( \frac{d\varphi_e}{dt} \right) (R + y_1), \\ V_{y_1} &= \left( \frac{dy_1}{dt} \right) + \left( \frac{d\varphi_e}{dt} \right) x_1, \\ V_{z_1} &= \left( \frac{dz_1}{dt} \right). \end{aligned} \quad (2)$$

The square of absolute payload  $M$  velocity may be written as  $V_{abs}^2 = V_{x_1}^2 + V_{y_1}^2 + V_{z_1}^2$ :

$$V_{abs}^2 = \left( \frac{dx_1}{dt} \right)^2 + \left( \frac{dy_1}{dt} \right)^2 + \left( \frac{dz_1}{dt} \right)^2$$

$$\begin{aligned}
 & + \left( \frac{d\varphi_e}{dt} \right)^2 (x_1^2 + (y_1 + R)^2) \\
 & + 2 \left( \frac{d\varphi_e}{dt} \right) \left( x_1 \left( \frac{dy_1}{dt} \right) - (y_1 + R) \left( \frac{dx_1}{dt} \right) \right) \\
 & = \left( \left( \frac{dx_1}{dt} \right) - \left( \frac{d\varphi_e}{dt} \right) (R + y_1) \right)^2 \\
 & + \left( \left( \frac{dy_1}{dt} \right) + \left( \frac{d\varphi_e}{dt} \right) x_1 \right)^2 + \left( \frac{dz_1}{dt} \right)^2.
 \end{aligned} \tag{3}$$

### 3. Dynamic Analysis

The slewing motion of the mechanical system “crane boom  $BO_2$ -load  $M$ ” in Figure 1 is governed by the vector equation for the rate of change of moment of momentum  $\mathbf{H}_3^{O_2}$  for the system “crane boom  $BO_2$ -load  $M$ ” with respect to point  $O_2$  in the inertial reference frame  $x_2y_2z_2$ :

$$\frac{d\mathbf{H}_3^{O_2}}{dt} = \sum \mathbf{M}^{O_2}. \tag{4}$$

The vector equation (4) contains the following components:

$$\mathbf{H}_3^{O_2} = I_{33}^{O_2} \boldsymbol{\omega}_e, \tag{5}$$

$$I_{33}^{O_2} = (I_{33}^{O_2})_{BO_2} + m(x_1^2 + (R + y_1)^2), \tag{6}$$

$$\sum \mathbf{M}^{O_2} = \mathbf{M}_{DT}^{O_2} - \mathbf{M}_{FT}^{O_2} = (M_{DT}^{O_2} - M_{FT}^{O_2}) \mathbf{k}, \tag{7}$$

where  $(I_{33}^{O_2})_{BO_2}$  is the element of mass moment of inertia for the crane boom  $BO_2$  in inertial fixed on earth reference frame  $x_2y_2z_2$  with respect to unit vector  $\mathbf{k}$  and  $m(x_1^2 + (R + y_1)^2)$  is the element of mass moment of inertia for the payload  $M$  in inertial fixed on earth reference frame  $x_2y_2z_2$  with respect to unit vector  $\mathbf{k}$ .

The external moment of gravitational force  $\mathbf{M}^{O_2}(\mathbf{mg}) = 0$  in (4) and (7) because  $\mathbf{mg} \updownarrow \mathbf{k}$ .

For the system “crane boom-payload,” the cable reaction force  $\mathbf{N}$  is the internal force. So in (4) and (7), we have  $\mathbf{M}^{O_2}(\mathbf{N}) = 0$ .

Substitution of (5), (6), and (7) into (4) yields the following scalar equation for the rate of change of moment of momentum  $H_3^{O_2}$  for the system “crane boom  $BO_2$ -load  $M$ ” with respect to point  $O_2$  in the inertial reference frame  $x_2y_2z_2$ :

$$\begin{aligned}
 & \frac{d}{dt} \left( \left( (I_{33}^{O_2})_{BO_2} + m(x_1^2 + (R + y_1)^2) \right) \left( \frac{d\varphi_e}{dt} \right) \right) \\
 & = M_{DT}^{O_2} - M_{FT}^{O_2},
 \end{aligned} \tag{8}$$

where driving  $M_{DT}^{O_2}$  and frictional  $M_{FT}^{O_2}$  torques are the technically defined functions for specific electric drive systems.

### 4. Nonlinear Mathematical Model with Lagrange Equations’ Introduction

Taking into account (3) for the square of absolute payload  $M$  velocity  $V_{abs}^2$ , and by adding the kinetic energy for a slewing crane boom according to (6), we will have the following expression for “crane boom-payload” kinetic energy:

$$\begin{aligned}
 T = \frac{m}{2} & \left( \left( \left( \frac{dx_1}{dt} \right) - \left( \frac{d\varphi_e}{dt} \right) (R + y_1) \right)^2 \right. \\
 & \left. + \left( \left( \frac{dy_1}{dt} \right) + \left( \frac{d\varphi_e}{dt} \right) x_1 \right)^2 + \left( \frac{dz_1}{dt} \right)^2 \right) \\
 & + \frac{I_{33}^{O_2}}{2} \left( \frac{d\varphi_e}{dt} \right)^2.
 \end{aligned} \tag{9}$$

For further analysis, we will assume that the crane boom slewing angular velocity is the constant  $d\varphi_e/dt = \omega_e$ . We will use the derived expression for kinetic energy for the left-hand sides of Lagrange equations in the noninertial reference frame  $x_1y_1z_1$ :

$$\begin{aligned}
 \frac{d}{dt} \left( \frac{\partial T}{\partial \dot{x}_1} \right) - \frac{\partial T}{\partial x_1} & = Q_{x_1}, \\
 \frac{d}{dt} \left( \frac{\partial T}{\partial \dot{y}_1} \right) - \frac{\partial T}{\partial y_1} & = Q_{y_1}, \\
 \frac{d}{dt} \left( \frac{\partial T}{\partial \dot{z}_1} \right) - \frac{\partial T}{\partial z_1} & = Q_{z_1}.
 \end{aligned} \tag{10}$$

Taking into account the nonlinearity and nonconservatism of the cable reaction force  $\mathbf{N}$ , we have the following formulae for the generalized forces in the noninertial reference frame  $x_1y_1z_1$ :

$$\begin{aligned}
 Q_{x_1} & = -N \left( \frac{x_1}{l} \right), \\
 Q_{y_1} & = -N \left( \frac{y_1}{l} \right), \\
 Q_{z_1} & = +N \left( \frac{l - z_1}{l} \right) - mg.
 \end{aligned} \tag{11}$$

Taking into account (9), (11), the equations (10) in the noninertial reference frame  $x_1y_1z_1$  will finally take the following form:

$$\begin{aligned}
 & m \left( \frac{d^2 x_1}{dt^2} \right) - m \left( \frac{d\varphi_e}{dt} \right)^2 x_1 - m \left( \frac{d^2 \varphi_e}{dt^2} \right) (R + y_1) \\
 & - 2m \left( \frac{d\varphi_e}{dt} \right) \left( \frac{dy_1}{dt} \right) = -N \left( \frac{x_1}{l} \right), \\
 & m \left( \frac{d^2 y_1}{dt^2} \right) - m \left( \frac{d\varphi_e}{dt} \right)^2 (R + y_1) + m \left( \frac{d^2 \varphi_e}{dt^2} \right) x_1 \\
 & + 2m \left( \frac{d\varphi_e}{dt} \right) \left( \frac{dx_1}{dt} \right) = -N \left( \frac{y_1}{l} \right),
 \end{aligned}$$

$$m \left( \frac{d^2 z_1}{dt^2} \right) = -mg + N \left( \frac{l - z_1}{l} \right),$$

$$l^2 = x_1^2 + y_1^2 + (z_1 - l)^2. \tag{12}$$

After two times differentiation of forth equations in system (12), we will have the following formula for the cable reaction force  $N$  (Figure 2) from third equation of (12):

$$N = \left( \left( ml \left[ \left( x_1 \left( \frac{d^2 x_1}{dt^2} \right) + \left( \frac{dx_1}{dt} \right)^2 \right. \right. \right. \right. \right. \right. \\ \left. \left. \left. + y_1 \left( \frac{d^2 y_1}{dt^2} \right) + \left( \frac{dy_1}{dt} \right)^2 \right) \right. \right. \\ \left. \left. \times (l^2 - x_1^2 - y_1^2) \right. \right. \\ \left. \left. + \left( x_1 \left( \frac{dx_1}{dt} \right) + y_1 \left( \frac{dy_1}{dt} \right) \right)^2 \right] \right) \tag{13} \\ \left. \times (l^2 - x_1^2 - y_1^2)^{-2} \right) \\ + \frac{mgl}{\sqrt{(l^2 - x_1^2 - y_1^2)}}.$$

So with an introduction of (13) to the first and second equations of system (12), we will have the explicit nonlinear ODE system for payload  $M$  swaying in Cartesian coordinates.

### 5. Linearized Mathematical Model

Further for the small angle  $\alpha_1$ , we may assume that  $z_1$  and  $d^2 z_1 / dt^2$  are the small parameters. So the nonlinear equation (13) yields

$$N \approx mg. \tag{14}$$

Then, taking into account (14), the linearized system (12) for the two variables  $x_1$  and  $y_1$  takes the following form:

$$\frac{d^2 x_1}{dt^2} - \left( \frac{d\varphi_e}{dt} \right)^2 x_1 - 2 \left( \frac{d\varphi_e}{dt} \right) \left( \frac{dy_1}{dt} \right) = -g \left( \frac{x_1}{l} \right),$$

$$\frac{d^2 y_1}{dt^2} - \left( \frac{d\varphi_e}{dt} \right)^2 (R + y_1) + 2 \left( \frac{d\varphi_e}{dt} \right) \left( \frac{dx_1}{dt} \right) = -g \left( \frac{y_1}{l} \right). \tag{15}$$

So we derive the system (15) of differential equations for relative motion of load  $M$  on cable  $BM$  with a movable suspension center  $B$ , which is fixed at the crane boom  $BO_2$ . We assume that the crane boom  $BO_2$  rotates with a constant angular velocity  $\omega_e$  around vertical axis  $DO_2$ . We then transfer the origin of coordinate system  $Oxy$  (Figure 1) to the point  $A_{dyn}$  of dynamic equilibrium for load  $M$  and assume that  $x_1 = x$ ;  $y_1 = y + y_{dyn}$  (Figure 3). Then, the second equation of system (15) defines the amount of dynamic deflection  $y_{dyn} = A_{st} A_{dyn} = (\omega_e^2 R l) / (g - \omega_e^2 l)$ .

Relative swaying paths of payload  $M$  in the plane of the introduced relative coordinates  $x$  and  $y$  are shown in Figure 3 for successive increasing swaying times  $t_1 = 1.25$  s (Figure 3(a)),  $t_2 = 3$  s (Figure 3(b)),  $t_3 = 10$  s (Figure 3(c)), and  $t_4 = 25$  s (Figure 3(d)).

Then, we have the normal system of two linear homogeneous differential equations of second order for relative motion of the load  $M$ :

$$\begin{pmatrix} D^2 - \left( \omega_e^2 - \left( \frac{g}{l} \right) \right) & -2\omega_e D \\ 2\omega_e D & D^2 - \left( \omega_e^2 - \left( \frac{g}{l} \right) \right) \end{pmatrix} \begin{pmatrix} x(t) \\ y(t) \end{pmatrix} = 0, \quad D = \frac{d}{dt}. \tag{16}$$

The determinant of natural frequencies matrix for the system (16) has the following form:

$$\begin{vmatrix} \lambda^2 + \left( \frac{g}{l} \right) - \omega_e^2 & -2 \cdot \omega_e \cdot \lambda \\ 2 \cdot \omega_e \cdot \lambda & \lambda^2 + \left( \frac{g}{l} \right) - \omega_e^2 \end{vmatrix} = 0. \tag{17}$$

Using (17), we adjust the roots  $\lambda_1$  and  $\lambda_2$  of secular equation:

$$\lambda_1 = \pm \nu_1 \cdot i, \quad \lambda_2 = \pm \nu_2 \cdot i, \quad \nu_1 = k + \omega_e, \tag{18} \\ \nu_2 = k - \omega_e, \quad k = \sqrt{\frac{g}{l}}, \quad \omega_e \neq k.$$

The initial conditions for the problem are as follows:

$$x(0) = 0, \quad Dx(0) = +V_B = +\omega_e R, \tag{19} \\ y(0) = -y_{dyn}, \quad Dy(0) = 0.$$

Taking into account (18) and (19), the law of relative motion for payload takes the following form:

$$x(t) = A_1 \frac{i}{2} (e^{-\nu_1 it} - e^{\nu_1 it}) + A_2 \frac{i}{2} (e^{-\nu_2 it} - e^{\nu_2 it}), \tag{20} \\ y(t) = A_1 \frac{1}{2} (e^{-\nu_1 it} + e^{\nu_1 it}) - A_2 \frac{1}{2} (e^{-\nu_2 it} + e^{\nu_2 it}).$$

After substitution of values of  $A_1$  and  $A_2$  in (20), we have the following law of payload  $M$  relative swaying motion with the uniformly rotating pivot center:

$$x(t) = \left( \frac{V_B - y_{dyn} (k - \omega_e)}{2k} \right) \frac{i}{2} (e^{-\nu_1 it} - e^{\nu_1 it}) \\ + \left( \frac{V_B + y_{dyn} (k + \omega_e)}{2k} \right) \frac{i}{2} (e^{-\nu_2 it} - e^{\nu_2 it}), \tag{21} \\ y(t) = \left( \frac{V_B - y_{dyn} (k - \omega_e)}{2k} \right) \frac{1}{2} (e^{-\nu_1 it} + e^{\nu_1 it}) \\ - \left( \frac{V_B + y_{dyn} (k + \omega_e)}{2k} \right) \frac{1}{2} (e^{-\nu_2 it} + e^{\nu_2 it}).$$

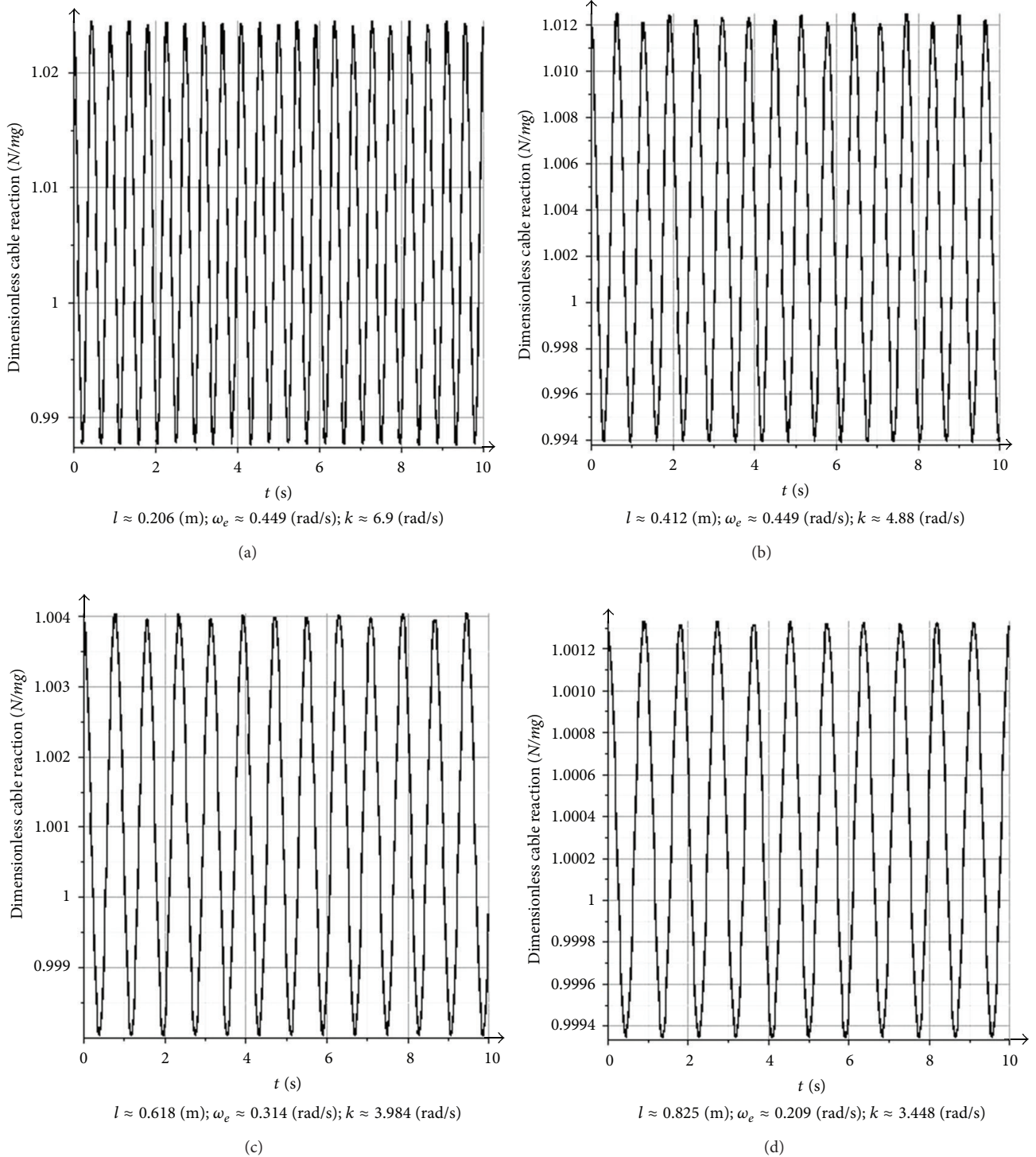


FIGURE 2: Time dependencies of dimensionless cable reactions  $N/mg$  in the first approximation for fixed cable lengths  $l = 0.206$  m (a);  $l = 0.412$  m (b);  $l = 0.618$  m (c); and  $l = 0.825$  m (d).

The relative trajectories for load  $M$  on the cable in Figure 3 have been derived for the following numerical values:  $R = 0.492$  m;  $g = 9.81$  m/s<sup>2</sup>;  $l = 0.825$  m;  $k = (g/l)^{0.5} \approx 3.448$  rad/s;  $T = 30$  s;  $\omega_e = 2\pi/T \approx 0.209$  rad/s;  $\alpha_{1dyn} = 0.00221$  rad;  $V_B = 0.103$  m/s;  $\gamma_{dyn} = 0.00182$  m;  $\nu_1 =$

$k + \omega_e = 3.658$  rad/s;  $\nu_2 = k - \omega_e = 3.239$  rad/s (Figure 3).

Numerical plots in Figure 3 show the payload  $M$  swaying in the noninertial reference frame ( $Oxyz$ ). In order to visualize payload  $M$  absolute swaying path (Figures 4 and 5)

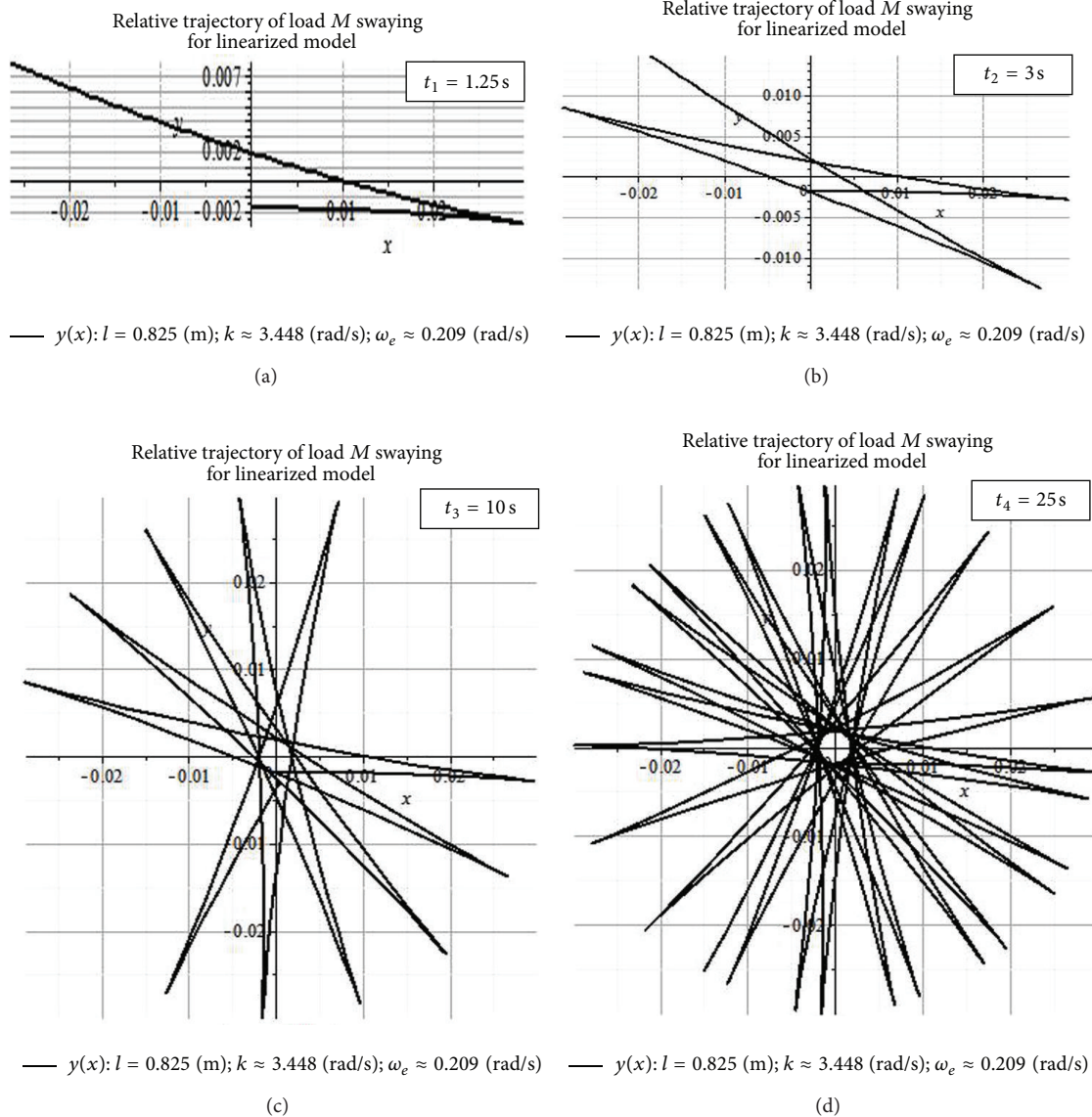


FIGURE 3: The relative trajectories for load M on the cable during uniform rotational motion of the crane boom  $BO_2$  for the moments of time  $t_1 = 1.25$  s (a),  $t_2 = 3$  s (b),  $t_3 = 10$  s (c), and  $t_4 = 25$  s (d).

in the fixed inertial reference frame  $(O_2x_2y_2z_2)$ , we will address the following transition formula:

$$\begin{pmatrix} x_2(t) \\ y_2(t) \end{pmatrix} = \begin{pmatrix} \sin(\omega_e t) & \cos(\omega_e t) \\ -\cos(\omega_e t) & \sin(\omega_e t) \end{pmatrix} \begin{pmatrix} x(t) \\ y(t) + R + y_{dyn} \end{pmatrix}. \quad (22)$$

Derived computational plot for absolute payload swaying path in the absolute coordinates' plane  $(x_2y_2)$  is shown in Figure 5(a) for load M swaying time  $t_1 = 15$  s and crane boom transport slewing angle  $\varphi_e = 180^\circ$ . In Figure 5(b), we show the experimental plot for absolute payload swaying path in the absolute coordinates' plane  $(x_2y_2)$  for load M swaying time  $t_2 = 15$  s and crane boom transport slewing angle  $\varphi_e = 180^\circ$ , which was built with an introduction of experimental setup in Figure 4.

## 6. Comparison of Derived and Known Published Results

The computational dimensionless cable force  $N/mg$ , derived in the first approximation and shown in Figure 2, outlines the minor change of the cable tension force in the vicinity of the ordinate  $(N/mg) = 1$ :  $(N/mg) \in [0.9875; 1.0233]$  for  $l = 0.206$  m in Figure 2(a);  $(N/mg) \in [0.994; 1.0122]$  for  $l = 0.412$  m in Figure 2(b);  $(N/mg) \in [0.998; 1.004]$  for  $l = 0.618$  m in Figure 2(c); and  $(N/mg) \in [0.99933; 1.0013]$  for  $l = 0.825$  m in Figure 2(d). So the assumption (14) really takes place as shown in Figure 2. The same effect for  $(N/mg)_{Mitre} \in [0.94; 1.04]$  has been derived by Mitrev and Grigorov, [23, Mitrev's Figure 7 in page 89], that confirms assumption (14). An analogous effect for dimensionless cable

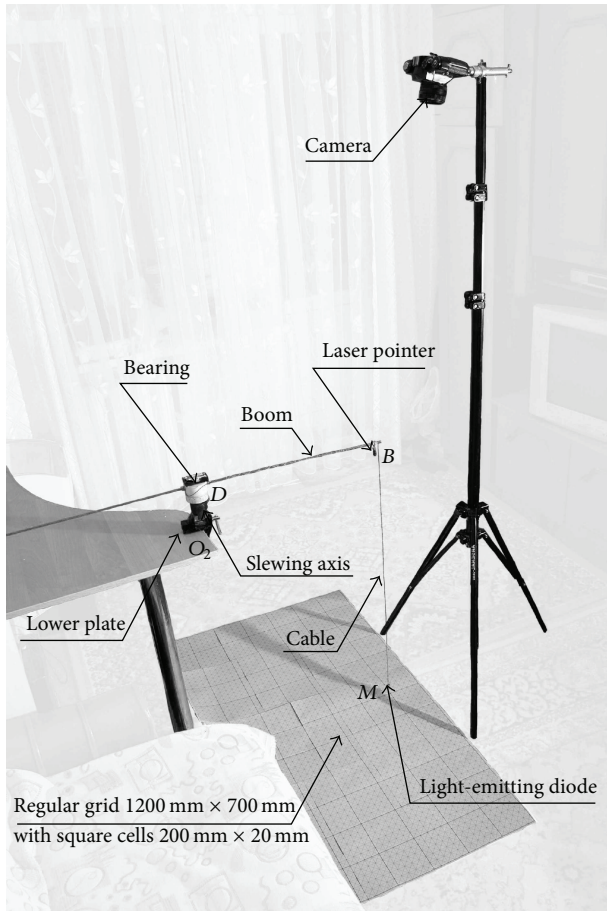


FIGURE 4: The experimental measurement system for payload  $M$  swaying during crane boom slewing.

force  $(N/mg)_{\text{Maczynski}} \in [0.996; 1.005]$  has been derived by Maczynski and Wojciech, [24, Maczynski's Figure 10 in page 278], which also reaffirms the assumption (14).

In published work by Sakawa et al. ([25], Figure 3 at page 552, Figure 4 at page 552, Figure 5 at page 554, and Figure 6 at page 554), the small Sakawa values  $dz/dt \leq 0.1$  (Figures 3 and 4) and  $dz/dt \leq 0.05$  (Figures 5 and 6) of  $z$ -projections for payload velocities have been shown, which confirms the small angle assumption  $N \approx mg$  (14).

## 7. Discussion and Analysis of Basic Results for Mathematical and Physical Simulation

The relative trajectories for load  $M$  swaying in Figure 3 show equality of maximum values for relative  $x$  and  $y$  payload coordinates:

$$x_{\max} = y_{\max} = A_1 + A_2 = \frac{\omega_e (R + y_{\text{dyn}})}{k}. \quad (23)$$

The formula (23) outlines that values  $x_{\max}$  and  $y_{\max}$  in Figure 3 increase with growth of boom slewing velocity  $\omega_e$

and with increased cable length  $l$ . The  $y_{\text{dyn}}$  influence on the values of  $x_{\max}$  and  $y_{\max}$  is negligible.

Equation (18) shows that the free oscillation frequencies  $\nu_1$  and  $\nu_2$  depend on the boom slewing velocity  $\omega_e$  and natural frequency  $k$  of the payload with a fixed pivot point  $B$ . The frequencies  $\nu_1$  and  $\nu_2$  essentially depend on the pendulum length  $l$  because  $k \gg \omega_e$ . Kinematically saying, the miscoordination of frequencies  $\nu_1$  and  $\nu_2$  is  $\nu_1 - \nu_2 = 2\omega_e$  and is determined by the crane boom slewing velocity  $\omega_e$ . Dynamically saying, the value of miscoordination is governed by the Coriolis acceleration-induced D'Alembert's inertia force.

Computations shown in Figure 3 for relative payload  $M$  swaying show that the clockwise direction of rotation for relative oscillations is opposite in direction from the counterclockwise direction of rotation for the crane boom. This effect follows from the conservation of position of the plane  $y_2z_2$  of oscillations of load  $M$  in the fixed inertial coordinate system  $x_2y_2z_2$ .

The comparative analysis of computational (1) and experimental (2) absolute payload trajectories is shown in Figure 5(c). The quantity of the local maximums in Figure 5(a) is 8 for theoretical curve 1. So the theoretical period for relative load swaying is  $T_{\text{theor}} = 1.87$  s. The quantity of the local maximums in Figure 5(b) is 7.5 for experimental curve 2. The period for experimental curve 2 in Figure 5(b) is  $T_{\text{experim}} = 2$  s. The discrepancy between the values of theoretical and experimental periods does not exceed 7%.

The experimental absolute trajectory (2) in Figures 5(b) and 5(c) outlines the additional relative swaying of payload  $M$  after crane boom stop, which has the elliptical form in the vicinity of the point  $(0, -0.5)$  in the plane  $x_2y_2$  for  $\varphi_e = 180^\circ$ . The remaining payload motions after crane boom stop are the small oscillations of the payload with the fixed pivot center.

## 8. Final Conclusions

The closed system of nonlinear ODEs for payload relative swaying has been derived in relative Cartesian coordinates with an introduction of Lagrange equations and a geometric constraint equation.

The explicit form of the dependence of the cable reaction force as a function of the relative payload coordinates  $x_1, y_1, z_1$  and their first and second time derivatives has been found. Derived complex dependency of the cable reaction force on the above mentioned variables determines the nonlinearity of the present problem.

The deviation of cable reaction force from payload gravity force is small. This fact allowed the derivation of a linearized ODE system for payload swaying in relative Cartesian coordinates and verified the small relative Cartesian coordinates' assumption. The analytical expressions for relative payload path have been derived.

Derived results have good agreement with experiments and known published data.



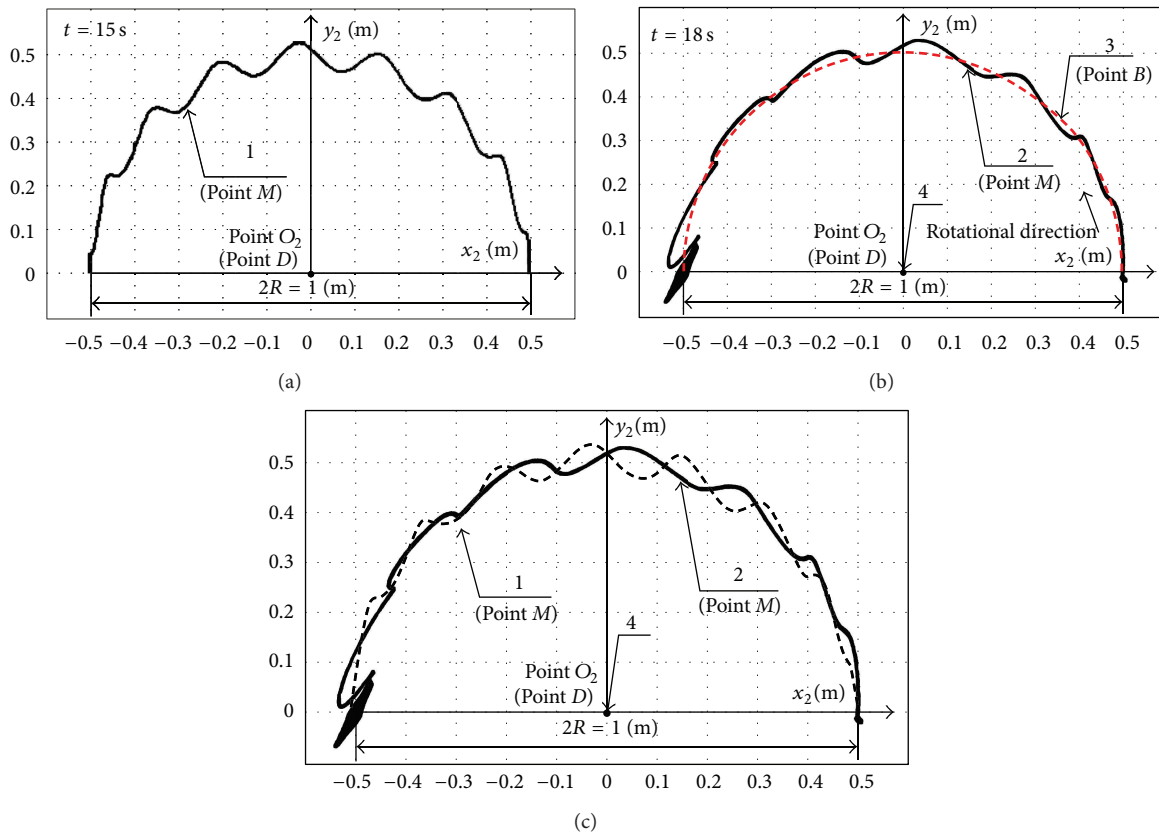


FIGURE 5: Calculated 1 (a, c) and experimental 2 (b, c) absolute trajectories for load  $M$ , where 3 is the trajectory of boom point  $B$  (b); 4 is the center  $O_2$  ( $D$ ) of boom rotation (b, c).

**Disclosure**

The submission of the authors’ paper implies that it has not been previously published, that it is not under consideration for publication elsewhere, and that it will not be published elsewhere in the same form without the written permission of the editors.

**Conflict of Interests**

The authors Alexander V. Perig, Alexander N. Stadnik, and Alexander I. Deriglazov declare that there is no conflict of interests regarding the publication of this paper.

**References**

[1] E. M. Abdel-Rahman and A. H. Nayfeh, “Pendulation reduction in boom cranes using cable length manipulation,” *Nonlinear Dynamics*, vol. 27, no. 3, pp. 255–269, 2002.

[2] W. Adamiec-Wójcik I, P. Fałat, A. Maczyński, and S. Wojciech, “Load stabilisation in an A-frame—a type of an offshore crane,” *The Archive of Mechanical Engineering*, vol. 56, no. 1, pp. 37–59, 2009.

[3] P. J. Aston, “Bifurcations of the horizontally forced spherical pendulum,” *Methods in Applied Mechanics and Engineering*, vol. 170, no. 3-4, pp. 343–3353, 1999.

[4] P. Betsch, M. Quasem, and S. Uhlar, “Numerical integration of discrete mechanical systems with mixed holonomic and control constraints,” *Journal of Mechanical Science and Technology*, vol. 23, no. 4, pp. 1012–1018, 2009.

[5] W. Blajer and K. Kołodziejczyk, “A geometric approach to solving problems of control constraints: theory and a DAE framework,” *Multibody System Dynamics*, vol. 11, no. 4, pp. 343–364, 2004.

[6] W. Blajer and K. Kołodziejczyk, “Control of underactuated mechanical systems with servo-constraints,” *Nonlinear Dynamics*, vol. 50, no. 4, pp. 781–791, 2007.

[7] W. Blajer and K. Kołodziejczyk, “Modeling of underactuated mechanical systems in partly specified motion,” *Journal of Theoretical and Applied Mechanics*, vol. 46, no. 2, pp. 383–394, 2008.

[8] W. Blajer and K. Kołodziejczyk, “The use of dependent coordinates in modeling and simulation of cranes executing a load prescribed motion,” *The Archive of Mechanical Engineering*, vol. 3, pp. 209–222, 2009, [http://ame.meil.pw.edu.pl/index.php?/eng/content/download/373/1748/file/art\\_2009\\_3\\_02.pdf](http://ame.meil.pw.edu.pl/index.php?/eng/content/download/373/1748/file/art_2009_3_02.pdf).

[9] W. Blajer, A. Czapllicki, K. Dziewiecki, and Z. Mazur, “Influence of selected modeling and computational issues on muscle force estimates,” *Multibody System Dynamics*, vol. 24, no. 4, pp. 473–492, 2010.

[10] W. Blajer and K. Kołodziejczyk, “Improved DAE formulation for inverse dynamics simulation of cranes,” *Multibody System Dynamics*, vol. 25, no. 2, pp. 131–143, 2011.

- [11] J. H. Cha, S. H. Ham, K. Y. Lee, and M. I. Roh, "Application of a topological modelling approach of multi-body system dynamics to simulation of multi-floating cranes in shipyards," *Proceedings of the Institution of Mechanical Engineers K*, vol. 224, no. 4, pp. 365–373, 2010.
- [12] K. Ellermann, E. Kreuzer, and M. Markiewicz, "Nonlinear dynamics of floating cranes," *Nonlinear Dynamics*, vol. 27, no. 2, pp. 107–183, 2002.
- [13] T. Erneux and T. Kalmár-Nagy, "Nonlinear stability of a delayed feedback controlled container crane," *Journal of Vibration and Control*, vol. 13, no. 5, pp. 603–616, 2007.
- [14] G. Glossiotis and I. Antoniadis, "Payload sway suppression in rotary cranes by digital filtering of the commanded inputs," *Proceedings of the Institution of Mechanical Engineers K*, vol. 217, no. 2, pp. 99–109, 2003.
- [15] R. A. Ibrahim, "Excitation-induced stability and phase transition: a review," *Journal of Vibration and Control*, vol. 12, no. 10, pp. 1093–1170, 2006.
- [16] J. Kortelainen and A. Mikkola, "Semantic data model in multibody system simulation," *Proceedings of the Institution of Mechanical Engineers K*, vol. 224, no. 4, pp. 341–352, 2010.
- [17] R. Mitrev, "Mathematical modelling of translational motion of rail-guided cart with suspended payload," *Journal of Zhejiang University Science A*, vol. 8, no. 9, pp. 1395–1400, 2007.
- [18] B. Grigorov and R. Mitrev, "A Newton—Euler approach to the freely suspended load swinging problem," *Recent Journal*, vol. 10, no. 26, pp. 109–112, 2009.
- [19] M. Osiński and S. Wojciech, "Application of nonlinear optimisation methods to input shaping of the hoist drive of an off-shore crane," *Nonlinear Dynamics*, vol. 17, no. 4, pp. 369–386, 1998.
- [20] H. L. Ren, X. L. Wang, Y. J. Hu, and C. G. Li, "Dynamic response analysis of a moored crane-ship with a flexible boom," *Journal of Zhejiang University Science A*, vol. 9, no. 1, pp. 26–31, 2008.
- [21] H. Schaub, "Rate-based ship-mounted crane payload pendulation control system," *Control Engineering Practice*, vol. 16, no. 1, pp. 132–145, 2008.
- [22] N. Uchiyama, "Robust control for overhead cranes by partial state feedback," *Proceedings of the Institution of Mechanical Engineers I*, vol. 223, no. 4, pp. 575–580, 2009.
- [23] R. Mitrev and B. Grigorov, "Dynamic behaviour of a spherical pendulum with spatially moving pivot," *Zeszyty Naukowe Politechniki Poznańskiej, Budowa Maszyn i Zarządzanie Produkcją*, vol. 9, pp. 81–91, 2008.
- [24] A. Maczynski and S. Wojciech, "Dynamics of a mobile crane and optimisation of the slewing motion of its upper structure," *Nonlinear Dynamics*, vol. 32, no. 3, pp. 259–290, 2003.
- [25] Y. Sakawa, Y. Shindo, and Y. Hashimoto, "Optimal control of a rotary crane," *Journal of Optimization Theory and Applications*, vol. 35, no. 4, pp. 535–557, 1981.



**Hindawi**

Submit your manuscripts at  
<http://www.hindawi.com>

